



Different dimensional coordination polymers with 4,4'-oxybis(benzoate): Syntheses, structures and properties

Huijie Lun^a, Yamin Li^{a,*}, Xudong Zhang^b, Jing-He Yang^a, Changyu Xiao^a, Yanqing Xu^{c,*}, Junrui Li^a

^a Henan Key Laboratory of Polyoxometalate; Institute of Molecular and Crystal Engineering, College of Chemistry and Chemical Engineering, Henan University, Kaifeng, Henan, 475004, PR China

^b State Key Laboratory of Structural Chemistry, Fujian Institute of Research on the Structure of Matter, Chinese Academy of Sciences, Fuzhou, Fujian 350002, PR China

^c School of Chemistry, Key Laboratory of Cluster Science, Ministry of Education of China, Beijing Institute of Technology, Beijing 100081, PR China

ARTICLE INFO

Article history:

Received 26 January 2014

Received in revised form

8 April 2014

Accepted 20 April 2014

Available online 26 April 2014

Keywords:

4,4'-oxydibenzoic acid

Hydrothermal condition

Luminescent properties

Magnetic property

ABSTRACT

Five transition-metal coordination polymers, namely, $[\text{Zn}_7\text{Cl}_6(\text{oba})_4]_n$ (**1**), $[\text{Cd}_7\text{Cl}_6(\text{oba})_4]_n$ (**2**), $[\text{Zn}(\text{oba})(\text{H}_2\text{O})]_n$ (**3**), $[\text{Ag}_2(\text{oba})]_n$ (**4**) and $[\text{Co}(\text{oba})(\text{H}_2\text{O})_2]_n$ (**5**) ($\text{H}_2\text{oba} = 4,4'$ -oxydibenzoic acid), have been achieved under hydrothermal conditions and structurally characterized by IR, elemental analyses, X-ray single-crystal diffraction and TGA. The X-ray single-crystal diffraction reveals that compounds **1** and **2** are isomorphism, featuring pillared-layer 3D motifs, in which the 2D inorganic layers $(\text{Zn}_6\text{Cl}_7)_n$ (or $(\text{Cd}_6\text{Cl}_7)_n$) are connected by oba^{2-} pillars. Compound **3** exhibits 1D stair-like chain and extends to a 3D network by two different interchain O–H–O hydrogen bonding interactions while compound **4** features wave chains and stretches to 2D layer by interchain Ag–O weak contacts. Compound **5** shows 2D network in which Co-chains are pillared by oba^{2-} ligand and then forms a 3D network by four different O–H–O hydrogen bonding interactions. Furthermore, **1–4** exhibit luminescent properties at a solid state and **5** shows antiferromagnetic behavior.

© 2014 Elsevier Inc. All rights reserved.

1. Introduction

In recent years, the transition-metal coordination polymers have received much attention not only because of their intriguing structures, but also for the potential applications in catalysis [1,2], separation and storage [3,4], optical properties [5], magnetism [6,7], etc. To construct desired transition-metal coordination polymers with rational and controllable structure, the self-assembly method is very frequently-used and is important in the synthesis. Moreover, selecting appropriate reaction conditions also plays a vital role, because many factors affect the formation, such as the metal ions, the pH value and the molar ratio of reactants, etc., especially the selection of organic ligands.

To the best of our knowledge, the aromatic carboxylate ligands have been widely used in the assembly process with their special advantages, in which the carboxyl groups can coordinate to metal ions through diverse coordination modes, such as terminal monodentate, chelating to one metal atom and bridging bidentate in different fashions [8]. Moreover, the carboxylate groups may be

completely or partially deprotonated, and can act as hydrogen bond acceptors as well as hydrogen bond donors to assemble supramolecular structures [9]; on the other hand, the existence of aromatic rings can promote the formation of π – π stacking interactions, which also play an important role in supramolecular networks. Further survey shows that, nowadays the utilization of aromatic carboxylate ligands that contain flexibility and rigidity such as 4,4'-oxydibenzoic acid, 4-(2-carboxyphenoxy)phthalic acid and so on has turned out to be a wise decision. Many compounds with interesting structures [10–14] and properties have been synthesized, for instance chiral [15], microporous [16], and luminescent [17] complexes. Encouraged by the factors, the V-shaped ligand 4,4'-oxydibenzoic acid catches our attention, which not only contains dicarboxylate groups and aromatic rings, providing acting sites for coordination and intermolecular forces, but also can twist or bend around the ether bond (the C–O–C angle is $121.8(4)^\circ$) [15] to meet the coordination requirements in the assembly process.

Herein, with H_2oba and triazines as starting materials, we obtained five coordination polymers, $[\text{Zn}_7\text{Cl}_6(\text{oba})_4]_n$ (**1**), $[\text{Cd}_7\text{Cl}_6(\text{oba})_4]_n$ (**2**) and $[\text{Zn}(\text{oba})(\text{H}_2\text{O})]_n$ (**3**), $[\text{Ag}_2(\text{oba})]_n$ (**4**) and $[\text{Co}(\text{oba})(\text{H}_2\text{O})_2]_n$ (**5**), which have different dimensions and structures. Meanwhile, the luminescent properties of **1–4** as well as magnetic property of **5** are also discussed in this paper.

* Corresponding authors. Tel./fax: +86378 3881589.

E-mail address: liyamin@henu.edu.cn (Y. Li).

2. Experimental

2.1. Materials and methods

All chemicals were commercially available and used as received without further purification. Infrared spectra were recorded on a Bruker VERTEX-70 FT-IR spectrophotometer using KBr pellets in the range of 400–4000 cm^{-1} . Elemental analyses were performed via Vario EL III Etro Elemental Analyzer. The fluorescent data were collected using a Hitachi Fluorescence spectrophotometer-F-7000. Magnetic measurement was carried out on a Quantum Design MPMS-XL SQUID magnetometer. Thermogravimetric analyses (TGA) were performed under N_2 atmosphere with a heating rate of 10 $^\circ\text{C min}^{-1}$ using TGA/SDTA851e. The X-Ray powder diffraction data were collected on Philips X'-PertPro diffractometer with Cu $K\alpha$ radiation.

2.2. Preparations of the compounds

2.2.1. Synthesis of $[\text{Zn}_7\text{Cl}_6(\text{oba})_4]_n$ (1)

ZnCl_2 (2 mmol, 0.272 g), H_2oba (1 mmol, 0.258 g), 2,4-diamino-6-phenyl-triazine (1 mmol, 0.187 g) and H_2O (8 mL) were added to Teflon-lined reactor and stirred for 20 min, and then kept at 180 $^\circ\text{C}$ for 3 days. After the autoclave had been cooled to room temperature over 6–7 h, colorless sheet crystalline solids of complex 1 (0.156 g, yield 36.8% based on oba^{2-}) were isolated from the mother liquid, washed with water. Anal. Calcd: $\text{C}_{56}\text{H}_{32}\text{Cl}_6\text{O}_{20}\text{Zn}_7$ (%): C, 39.68; H, 1.90. Found: C, 39.43; H, 2.12. IR (KBr pellet, cm^{-1}): 3436(m), 1595(s), 1537(m), 1359(s), 1261(s), 1161(m), 880(w), 854(w), 787(m), 695(w), 659(w).

2.2.2. Synthesis of $[\text{Cd}_7\text{Cl}_6(\text{oba})_4]_n$ (2)

Replacement of ZnCl_2 of 1 by $\text{CdCl}_2 \cdot 2.5\text{H}_2\text{O}$, 2,4-diamino-6-phenyl-triazine by 2,4-diamino-6-chlorine-triazine, colorless sheet crystalline solids of complex 2 (0.208 g, yield 41.1% based on oba^{2-}) were isolated from the mother liquid, washed with water. Anal. Calcd: $\text{C}_{56}\text{H}_{32}\text{Cl}_6\text{O}_{20}\text{Cd}_7$ (%): C, 33.22; H, 1.59. Found: C, 35.54; H, 1.73. IR (KBr pellet, cm^{-1}): 3442(s), 1596(s), 1536(m), 1360(s), 1261(s), 1160(m), 881(w), 856(w), 785(m), 697(w), 659(w).

2.2.3. Synthesis of $[\text{Zn}(\text{oba})(\text{H}_2\text{O})]_n$ (3)

Replacement of 2,4-diamino-6-phenyl-triazine of 1 by 2,4-diamino-6-methyl-triazine, colorless block crystalline solids of complex 3 (0.084 g, yield 24.7% based on oba^{2-}) were isolated from the mother liquid, washed with water. Anal. Calcd: $\text{C}_{14}\text{H}_{10}\text{O}_6\text{Zn}$ (%): C, 49.51; H, 2.97. Found: C, 49.37; H, 3.21. IR (KBr pellet, cm^{-1}): 3362(m), 1597(s), 1542(s), 1400(s), 1304(w), 1253(s), 1162(s), 880(m), 783(m), 697(w), 668(m).

2.2.4. Synthesis of $[\text{Ag}_2(\text{oba})]_n$ (4)

When the metal salt AgNO_3 was used to replace ZnCl_2 of 1, yellow block crystalline solids of complex 4 (0.062 g, yield 13.1% based on oba^{2-}) were isolated from the mother liquid, washed with water. Anal. Calcd: $\text{C}_{14}\text{H}_8\text{O}_5\text{Ag}_2$ (%): C, 35.73; H, 1.71. Found: C, 35.53; H, 1.91. IR (KBr pellet, cm^{-1}): 3409(m), 3232(m), 1592(s), 1543(s), 1396(s), 1259(s), 1157(m), 887(w), 828(w), 776(w), 660(w).

2.2.5. Synthesis of $[\text{Co}(\text{oba})(\text{H}_2\text{O})_2]_n$ (5)

By replacement of ZnCl_2 and 2,4-diamino-6-phenyl-triazine of 1 by $\text{CoCl}_2 \cdot 6\text{H}_2\text{O}$ and 2,4-diamino-6-vinyl-triazine and the temperature were maintained at 150 $^\circ\text{C}$, purple sheet crystalline solids of complex 5 (0.142 g, yield 40.4% based on oba^{2-}) were isolated from the mother liquid, washed with water. Anal. Calc: $\text{C}_{14}\text{H}_{12}\text{O}_7\text{Co}$ (%): C, 47.86; H: 3.45. Found: C: 47.88; H: 3.44. IR (KBr pellet, cm^{-1}):

3589(m), 3179(m), 1600(s), 1500(m), 1428(s), 1396(s), 1259(s), 1158(m), 1102(w), 872(w), 778(w), 658(w).

2.3. X-ray crystallographic analyses

X-ray single crystal data were collected at 296(2) K (for 1–5) on a Bruker Apex-II CCD area detector diffractometer with Mo $K\alpha$ radiation ($\lambda = 0.71073 \text{ \AA}$). Data reduction and absorption correction were made with empirical methods. The structures were solved by direct methods using SHELXS-97 [18] and refined by full-matrix least-squares techniques using SHELXL-97 [19]. Anisotropic displacement parameters were refined for all non-hydrogen atoms. And all hydrogen atoms bonded to C atoms were added in the riding model while the aqueous hydrogen atoms of 3 and 5 were located from the difference Fourier maps. The crystal data and refinement details for five complexes are shown in Table 1 and selected bond lengths (\AA) and bond angles ($^\circ$) in (Table S1 In supporting information). CCDC numbers 944947, 944948, 944946, 977122 and 977121 for compounds 1–5, respectively. These crystallographic data for this paper can be obtained free of charge via www.ccdc.cam.ac.uk/conts/retrieving.html (or from the Cambridge Crystallographic Data Centre, 12 Union Road, Cambridge CB2 1EZ, UK; fax: (+44) 1223-336-033; or e-mail: deposit@ccdc.cam.ac.uk).

3. Results and discussions

3.1. Syntheses

Under the similar synthesis conditions, much effort had been put to get other crystals with different metal salts but it failed and only the precipitates were present. It is inferred that the conditions such as the pH value or reacting temperature might be not suitable for crystallization of other compounds [20]. In the synthesized compounds, though the triazines are absent, their roles in adjusting the pH value cannot be neglected. It is probable that the $-\text{NH}_2$ groups of triazines and the carboxyl groups of H_2oba form a buffer solution, which can adjust the pH value in a small scope, providing a suitable condition for crystals [21].

3.2. Crystal structures of compounds 1 and 2

Single-crystal X-ray diffraction analyses reveal that compounds 1 and 2 are isomorphous, crystallizing in triclinic system $P-1$ space group, featuring pillared-layer 3D motifs, in which the 2D inorganic layers $(\text{Zn}_6\text{Cl}_7)_n$ (or $(\text{Cd}_6\text{Cl}_7)_n$) are further connected by oba^{2-} pillars. The asymmetric unit of 1 consists of four crystallographically independent zinc atoms, three chlorine atoms and two oba^{2-} ligands. The coordination environment around four zinc atoms is shown in Fig. 1a, Zn1, Zn2 and Zn3 atoms possessing distorted octahedral geometrical configuration and Zn4 in a square-pyramidal configuration. The Zn1 atom is coordinated to three oxygen atoms from three oba^{2-} ligands, and three chlorine atoms. The Zn2 and Zn3 atoms, however, are coordinated to four oxygen atoms from four oba^{2-} ligands, and two chlorine atoms. The Zn4 atom is coordinated to three oxygen atoms from three oba^{2-} ligands and one chlorine atom at basal face and the other at apical site. The Zn–Cl lengths are in the range from 2.581(3) \AA to 2.688(3) \AA , similar distances of which from 2.3678(17) \AA to 2.6710(19) \AA are ever observed in reported compound $[\text{Zn}_2(\text{EM}5)(\mu\text{-Cl})_3]_2(\text{ClO}_4)_2 \cdot 4\text{H}_2\text{O}$ (EM=bis(1,4,7-triazacyclononane)) [22]. The Zn–O lengths are in the range from 2.209(7) \AA to 2.392(7) \AA . Zn2 sitting at a center of inversion is connected to two Zn3 atoms (Zn3 and Zn3A, A: $1-x, 1-y, -z$) and two Zn4 atoms (Zn4B and Zn4C, B: $2-x, 1-y, -z$; C: $-1+x, y, z$) by two μ_3 -Cl atoms. And then the two pairs of zinc atoms are further connected to two Zn1 atoms

Table 1
Crystal data and refinement details for compounds 1–5.

	1	2	3	4	5
Empirical formula	C ₅₆ H ₃₂ Cl ₆ O ₂₀ Zn ₇	C ₅₆ H ₃₂ Cl ₆ O ₂₀ Cd ₇	C ₁₄ H ₁₀ O ₆ Zn	C ₁₄ H ₈ O ₅ Ag ₂	C ₁₄ H ₁₂ O ₇ Co
Formula weight	1695.11	2024.32	339.5	471.94	351.17
Crystal system	Triclinic	Triclinic	Monoclinic	Orthorhombic	Monoclinic
Space group	<i>P</i> -1	<i>P</i> -1	<i>P</i> 2 ₁ / <i>c</i>	<i>P</i> bcn	<i>P</i> 2 ₁ / <i>c</i>
<i>a</i> (Å)	10.3682(12)	10.3615(8)	14.1474(15)	7.2411(12)	13.883(6)
<i>b</i> (Å)	10.7642(12)	10.7636(8)	16.0945(17)	5.6063(9)	9.869(5)
<i>c</i> (Å)	15.1820(17)	15.1561(10)	5.9044(7)	29.614(5)	10.132(4)
α (°)	85.909(2)	85.9550(10)	90.00	90.00	90.00
β (°)	74.367(2)	74.3650(10)	97.402(2)	90.00	104.198(10)
γ (°)	61.995(2)	62.0070(10)	90.00	90.00	90.00
<i>V</i> (Å ³)	1437.6(3)	1434.21(18)	1333.2(3)	1202.2(3)	1345.8(10)
<i>Z</i>	1	1	4	4	4
<i>T</i> (K)	296(2)	296(2)	296(2)	296(2)	296(2)
μ (mm ⁻¹)	3.228	2.903	1.867	3.277	1.310
<i>D_c</i> (g/cm ³)	1.958	2.344	1.692	2.608	1.733
θ limits (°)	2.15 to 25.00	1.40 to 25.00	1.45 to 28.26	3.13 to 24.99	2.56 to 24.99
Ref. collected	4999	5005	3187	1057	2358
Ref. unique	4311	4518	2402	935	1322
<i>R</i> _{int}	0.0230	0.0224	0.0235	0.0241	0.1126
<i>R</i> index [<i>I</i> > 2 σ (<i>I</i>)]	<i>R</i> ₁ = 0.0799, <i>wR</i> ₂ = 0.2331	<i>R</i> ₁ = 0.0301, <i>wR</i> ₂ = 0.0804	<i>R</i> ₁ = 0.0323, <i>wR</i> ₂ = 0.0878	<i>R</i> ₁ = 0.0339, <i>wR</i> ₂ = 0.834	<i>R</i> ₁ = 0.0760, <i>wR</i> ₂ = 0.1628
<i>R</i> (all data)	<i>R</i> ₁ = 0.0867, <i>wR</i> ₂ = 0.2438	<i>R</i> ₁ = 0.0345, <i>wR</i> ₂ = 0.0888	<i>R</i> ₁ = 0.0531, <i>wR</i> ₂ = 0.1070	<i>R</i> ₁ = 0.0387, <i>wR</i> ₂ = 0.086	<i>R</i> ₁ = 0.1432, <i>wR</i> ₂ = 0.1901
GOOF	1.060	1.052	1.087	1.075	0.981
$\Delta\rho_{\max}$ (eÅ ⁻³)	-2.676	-1.837	-0.494	-1.200	-0.521
$\Delta\rho_{\min}$ (eÅ ⁻³)	0.291	0.396	0.146	0.106	0.129

$R = \sum(|F_o| - |F_c|) / \sum |F_o|$, $wR = \{ \sum w[(F_o^2 - F_c^2)^2] / \sum w[(F_o^2)^2] \}^{1/2}$, $w = 1 / [\sigma^2(F_o^2) + (aP)^2 + bP]$, $P = (F_o^2 + 2F_c^2) / 3$ [0]. **1**: *a* = 0.1901, *b* = 3.1900; **2**: *a* = 0.0547, *b* = 0.000; **3**: *a* = 0.0590, *b* = 0.000; **4**: *a* = 0.0340, *b* = 6.1993; **5**: *a* = 0.0615, *b* = 0.000.

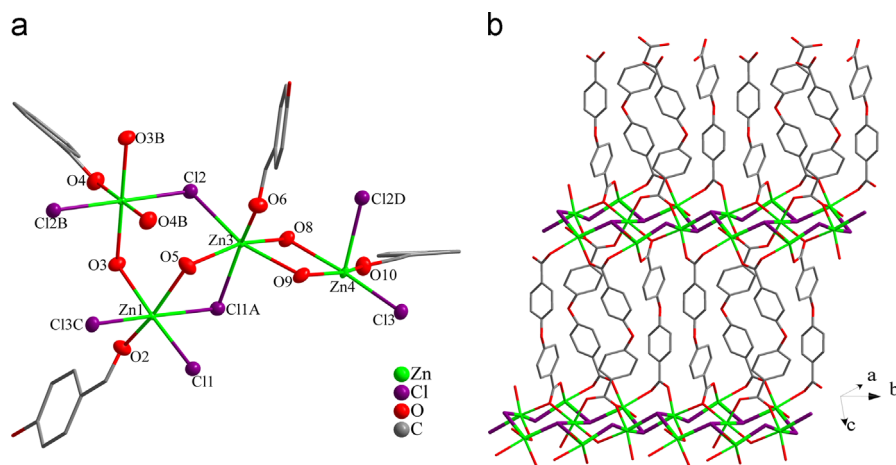


Fig. 1. (a) An ORTEP drawing of compound **1** showing 30% ellipsoid probability (A: 1-*x*, 2-*y*, -*z*; B: 1-*x*, 1-*y*, -*z*; C: -1+*x*, *y*, *z*; D: 2-*x*, 1-*y*, -*z*); (b) the 3D pillared-layer structure of **1**.

through two μ_3 -Cl and two μ_2 -Cl atoms, furnishing [Zn₇Cl₆] unit. Such unit is rare in the reported coordination polymers containing Zinc and Chlorine atoms. The adjacent units are doubly linked by two Zn1-Cl1 bonds (Zn1-Cl1 = 2.623 Å), resulting in one-dimensional chain (Fig. S1). Weak Zn-Cl contacts have also been found to extend the chains into 2D sheet (Zn-Cl = 2.884 Å), giving rise to 2D [Zn₇Cl₆]_n inorganic sheet (Fig. S2). The adjacent layers are pillared by oba²⁻ ligand to form a 3D structure with an interlayer Zn-Zn distance of ca. 15.182 Å, which adopts μ_6 - η^1 : η^2 : η^1 : η^2 mode (Fig. 1b). As the linker, the ether-oxygen angles (C-O-C) of oba²⁻ are 120.3° and 120.2°.

Though many 3D pillared-layer compounds have been obtained [23–25], the 2D layers of them are mostly formed by metal-hydroxide layers such as compound α -Cd₂(μ_3 -OH)₂(2,4-pyda) (2,4-pydaH₂ = 2,4-pyridinedicarboxylic acid) [26], [(Mn(OH)₂)(C₁₂H₈O(COO)₂)₂] [(C₁₂H₈O(COO)₂)₂] = oba²⁻ = 4,4'-oxybis(benzoate)) [27]

and so on, which are further pillared by organic ligand to 3D networks. While in compounds **1** and **2**, the 2D inorganic layers are comprised by metal-chlorine units and then stretch to 3D networks by organic linkers, which appear to be not common.

3.3. Crystal structure of compound 3

Compound **3** crystallizing in monoclinic *P*2₁/*c* space group exhibits 1D stair-like chain built up from binuclear zinc units by oba²⁻ ligands. As shown in Fig. 2a, the binuclear unit contains two symmetrical Zn(II) ions, both of which bear distorted tetrahedral geometry, ligated by three oxygen atoms from three oba²⁻ ligands and another oxygen atom from one water molecule. The Zn-O lengths are in the range of 1.959(2) to 2.010(2) Å and O-Zn-O angles from 98.15(9)° to 134.54(9)°. Both lengths and angles are comparable to the reported compound Zn₂(oba)₂ [15]. In addition,

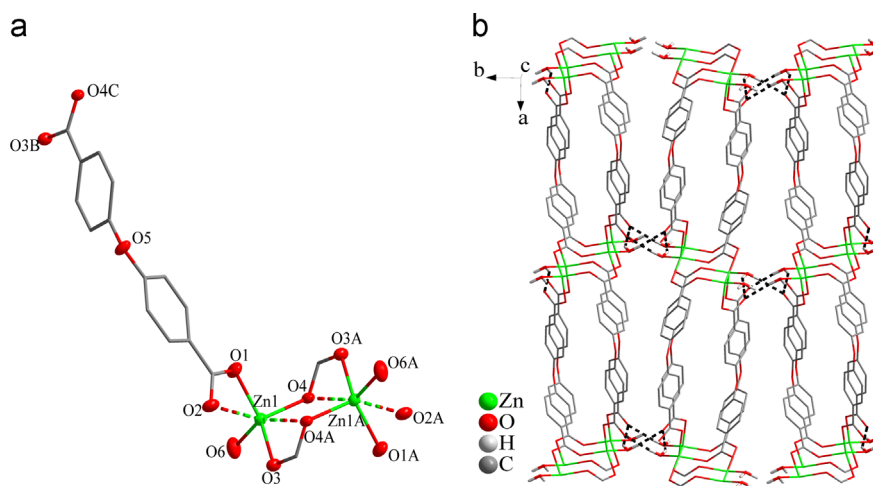


Fig. 2. (a) Binuclear zinc unit of compound **3**, the atom showing 30% ellipsoid probability (A: $2-x, -y, -z$; B: $-1+x, y, z$; C: $1-x, -y, -z$); (b) the 3D network structure of **3** by hydrogen bond interactions.

each Zn atom possesses two weak interactions with carboxylate-oxygen atoms with the separation of Zn–O between 2.681 and 2.790 Å, which are a little longer than the common Zn–carboxyl distance [28]. Zn1 and Zn1A (A: $2-x, -y, -z$) atoms are bridged by two *syn,anti*- μ_2 - η^1 : η^1 carboxylate groups into binuclear unit with Zn–Zn distance of 3.813 Å. Then the binuclear units are further linked by two *oba*²⁻ ligands using μ_3 - η^1 : η^1 : η^1 mode (ignoring Zn–O weak interactions), resulting in one-dimensional stair-like chains (Fig. S3), similar structure ever observed in compound $\{[\text{Ag}_2(\text{D-Hasp})(\text{L-Hasp})] \cdot 1.5\text{H}_2\text{O}\}_n$ (H_2asp =aspartic acid) [29]. Due to the diverse coordination modes of *oba*²⁻, different structures are observed in reported compound $[\text{Zn}(\text{oba})(\text{H}_2\text{O})]$ [30] with the same formula from compound **3**, of which two carboxylate moieties of *oba*²⁻ bridge each Zn center to produce 1D (Zn–*oba*)_n chains and are further connected by the *oba*-frameworks to yield a 2D structure. In the ligand *oba*²⁻ of compound **3**, C–O–C angle is about 120.0° and the angle of two phenyl rings is about 63.32°, smaller than the literature reported 65.1° [12] and 66.5° [16].

In addition, between adjacent one-dimensional stair-like chains, there exist two O–H–O hydrogen bonding interactions between coordination water molecules and carboxyl oxygen atoms of *oba*²⁻ ligands, which are O6–H6–O2#1, 2.864 Å; O6–H6B–O2#2, 2.879 Å (#1: $x, y, z+1$; #2: $x, -y+1/2, z+1/2$) (Table S2 in supporting information:), and as a result, the whole 3D supramolecular network is built up (Fig. 2b).

3.4. Crystal structure of compound 4

With crystallizing in orthorhombic system *Pbcn* space group, the compound **4** exhibits wave chains consisting of binuclear silver units bridged by *oba*²⁻ ligands and then connects to a two-dimensional network by Ag–O weak interactions. As shown in Fig. 3a, in binuclear silver unit, Ag1 and Ag1A (A: $1-x, -y, 1-z$) are symmetrical, and clamped by two *syn, syn*- μ_2 - η^1 : η^1 carboxyl groups from two *oba*²⁻ ligands, resulting in a $[\text{Ag}_2\text{C}_2\text{O}_4]$ eight-membered ring, similar coordination mode of carboxyl group has been observed in compounds $[\text{Ag}_2(\text{NO}_2\text{-bdc})(\text{phdat})]_n$ (*phdat*=2,4-diamine-6-phenyl-1,3,5-triazine) [31] and $[\text{Ag}(\text{bga})_2(\text{tpa})_{0.5}]_n$ (*bga*=benzoguanamine, H_2tpa =terephthalic acid) [32]. The distance of Ag–Ag is 2.876 Å, significantly shorter than twice the Vander Waals radius of Ag(I) (3.40 Å), and even shorter than Ag–Ag contact in metallic silver (2.89 Å), which suggests the existence of argentophilicity can enhance the aggregation of silver atoms [33]. Each silver atom is coordinated to two oxygen atoms from

two *oba*²⁻ ligands with Ag–O lengths in the range of 2.155(3)–2.185(3) Å, the O–Ag–O angle 159.96°, which is comparable with those reported silver carboxylate compounds [34,35]. The binuclear silver units are further bridged by *oba*²⁻ with a μ_4 - η^1 : η^1 : η^1 : η^1 mode forming 1D infinite wave chains. Besides, each silver atom exhibits additional contact to one oxygen atom from *oba*²⁻ ligand between chains with Ag–O distance of 2.625 Å, similar weak contact ever observed in the compound $[\text{Ag}_5(\text{nda})_2.5(\text{dmt})]_n$ (H_2nda =naphthalene-1,4-dicarboxylic acid, *dmt*=2,4-diamine-6-methyl-1,3,5-triazine) [20] with Ag–O distance between 2.617 and 2.878 Å, in virtue of which, the one-dimensional wave chains are extended into two-dimensional network (Fig. 3b). The angle of the two aromatic rings of *oba*²⁻ ligand is 57.034°.

3.5. Crystal structure of compound 5

Single-crystal X-ray analysis reveals that compound **5**, which crystallizes in monoclinic space group *P2₁/c*, is a three-dimensional coordination polymer formed by hydrogen bonding interactions. As shown in Fig. 4a, the asymmetrical unit of compound **5** contains one cobalt atom, one *oba*²⁻ ligand and two coordinated water molecules. Co1 atom is coordinated to six oxygen atoms, four from three *oba*²⁻ ligands and the other two from two water molecules, resulting in distorted octahedral geometry. The Co–O lengths are ranging from 2.014(5) Å to 2.175(5) Å, which are in the normal range of Co–carboxyl compounds [36,37]. In compound **5**, the neighboring cobalt atoms are linked into one-dimensional infinite chain via *syn,anti*- μ_2 - η^1 : η^1 carboxyl groups with Co–Co distance of 5.21 Å, and further connected to two-dimensional layer structure by pillared ligand *oba*²⁻, which adopts μ_3 - η^1 : η^1 : η^1 : η^1 modes (Fig. S4). While in the reported compound $[\text{Co}(\text{Hoba})_2(\text{H}_2\text{O})_2]$ [38], only one carboxylic acid of each H_2oba ligand is deprotonated, and $\text{Co}(\text{Hoba})_2$ layers are formed due to different coordination modes of H_2oba^- . The dihedral angle of the two aromatic rings connected by the ether oxygen atom in compound **5** is 79.253°, larger than the dihedral angles of four compounds described above in this paper.

In addition, the 2D layer framework is stabilized by an intra-layer O–H–O hydrogen bonding interaction between water molecules and *oba*²⁻ ligands, with the oxygen atoms from *oba*²⁻ ligand acting as acceptor (O6–H6B–O4#1 (#1: $x, y, z+1$)). Then three dimensional supramolecular networks are further formed via three inter-layer hydrogen bonding interactions, which are O6–H6C–O2#2, O7–H7B–O1#3, O7–H7C–O2#2 (#2: $-x, y-1/2, -z-1/2$; #3: $-x, -y, -z$) (Fig. 4b and Table S2 in supporting information).

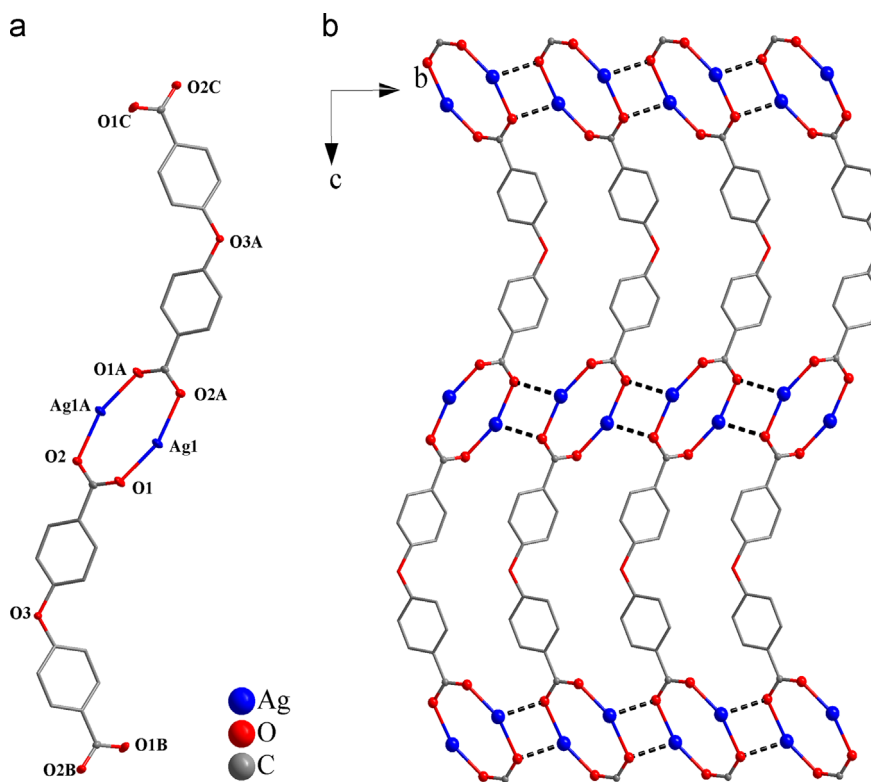


Fig. 3. (a) Binuclear silver unit of compound **4**, the atoms showing 30% ellipsoid probability (A: $1-x, -y, 1-z$); (b) the 2D network of compound **4** connected by Ag–O weak contacts.

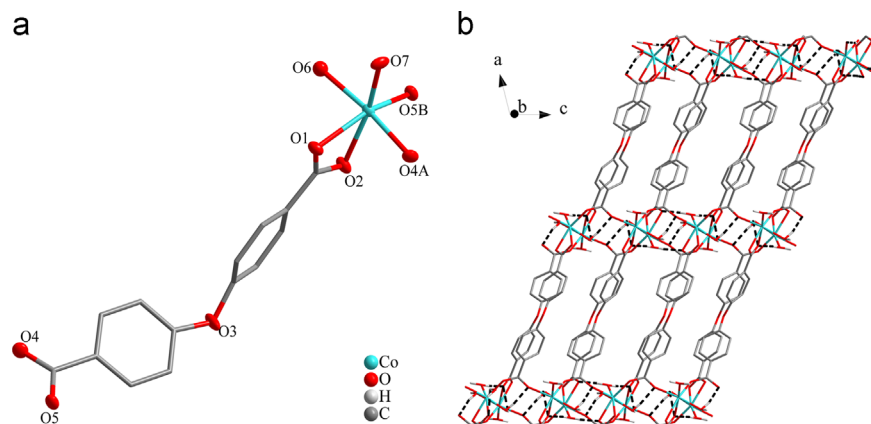


Fig. 4. (a) The asymmetrical unit of compound **5**, atoms showing 30% ellipsoid probability; (b) the 3D structure of **5** by hydrogen bond interactions.

3.6. IR spectra

The IR spectra of 1–5 display the characteristic absorption bands of H₂oba. The strong peaks of 1595 cm⁻¹, 1359 cm⁻¹ for 1, 1596 cm⁻¹, 1360 cm⁻¹ for 2, 1597 cm⁻¹, 1400 cm⁻¹ for 3, 1592 cm⁻¹, 1396 cm⁻¹ for 4, 1600 cm⁻¹, 1396 cm⁻¹ for 5 can be attributed to the asymmetric (ν_{as}) and symmetric (ν_s) stretching vibration of carboxyl groups, respectively, indicating the ligand H₂oba has been coordinated to different metal ions in bridging fashion [20]. The bands 600–900 cm⁻¹ can be attributed to the stretching of C–H of benzene ring (Fig. S5 in supporting information).

3.7. XRD and thermal stability

In order to confirm the phase purities of compounds 1–5, the X-ray powder diffraction of these compounds was characterized at

room temperature. As shown in Fig. S6, the peak positions of simulated and experimental curves are in good agreement with each other, suggesting that the crystal samples are pure.

The thermogravimetric analyses (TGA) were performed under N₂ atmosphere and the TG curves are shown in Fig. S7. For compounds 1 and 2, the stabilities are high from the observed, which are evident from the beginning loss temperature (about 350 °C). The curves are close to zero at 800 °C suggesting the nearly complete weight loss of 1 and 2, which can be attributed to the sublimation of newly formed MCl₂ (M=Zn, Cd) compounds [39,40]. Two-step weight loss is observed of compound 3 that the first loss of 6.2% (calc. 5.3%) at 160–360 °C, corresponding to the removal of one coordinated water molecule, while the second loss at 400–530 °C is for the framework collapse. The compound 4 loses oba²⁻ ligand at about 300 °C, and the remaining weight 51.1% (calc. 50.9%) indicates the final product is Ag₂O. As for compound 5, the first loss of 10.72% (calc. 10.26%) is at approximately 100 °C,

in accordance with the removal of two coordinated water molecules; the residues can be thermally stable to 370 °C.

3.8. Luminescent properties of compound 1–4

The room-temperature photoluminescence spectra of compounds 1–4 are shown in Fig. 5. The free ligand H₂oba displays photoluminescence with the emission maximum at 319 nm ($\lambda_{\text{ex}}=276$ nm, Fig. S8), which can be presumed that the peak originates from the $\pi^* \rightarrow \pi$ transition [41]. For compounds 1 and 2, upon the excitation of 280 nm, emissions are observed between 335 and 326 nm, respectively, while the emission of 338 nm ($\lambda_{\text{ex}}=278$ nm) is shown in compound 3, all of which can be assigned to intraligand ($\pi^* \rightarrow \pi$) transition [42]. For Zn(II) and Cd(II) ions, it is difficult to oxidize or to reduce owing to the d¹⁰ configuration, emissions are neither ligand-to-metal charge transfer (LMCT) nor metal-to-ligand charge transfer (MLCT) [43]. With regard to compound 4, two peaks of 360 nm and 494 nm are observed, and the former can be attributed to intraligand ($\pi^* \rightarrow \pi$) transition, while the latter may be assigned to the ligand-to-metal charge transfer (LMCT) bands [44,45]. As we know, many Ag(I) complexes are emissive only at a low temperature owing to the intense spin-orbital coupling of Ag(I), and the room-temperature photoluminescent Ag(I) complexes that are scarce [46]. Therefore, compound 4 may be a promising candidate for photo-active materials.

3.9. Magnetic property of compound 5

The temperature dependence magnetic susceptibility data of compound 5 is measured for crystal sample under an applied field of 1000 Oe in the range of 2–300 K. The plots of $\chi_m T$ and χ_m^{-1} are shown in Fig. 6. The $\chi_m T$ value is 3.08 cm³ mol⁻¹ K at 300 K, which is larger than the expected (1.875 cm³ mol⁻¹ K) for one isolated Co(II) ion ($S=3/2$, $g=2.0$), owing to the orbital contribution of Co(II) in an octahedral environment [47]. Upon cooling, the value steadily decreases to reach the value of 2.31 cm³ mol⁻¹ K at 50 K, and sharply decreases to the value of 0.43 cm³ mol⁻¹ K at 2 K on further cooling, which show the existence of antiferromagnetic exchange interactions between Co(II) ions. The χ_m^{-1} vs. T plot is well fitted by the Curie-Weiss law $\chi=C/(T-\theta)$ in the temperature 300–25 K, with the Weiss temperature $\theta=-15.19$ K and Curie constant $C=3.13$ cm³ mol⁻¹ K, which is consistent with the presence of hexacoordinated high-spin Co(II) ions ($C=2.8$ – 3.4 cm³ mol⁻¹ K) [48,49]. The negative θ value further confirms the antiferromagnetic behavior.

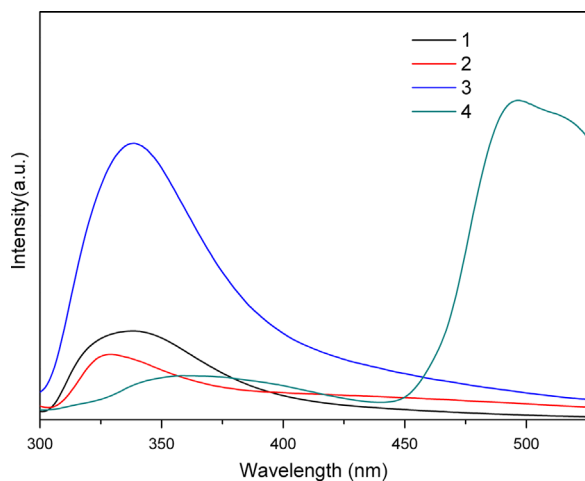


Fig. 5. The emission spectra of compounds 1–4 at solid state.

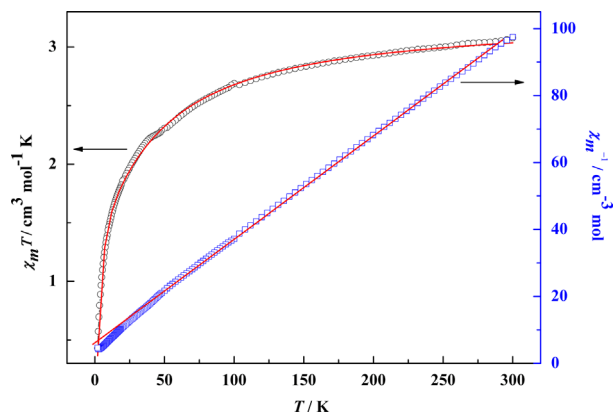


Fig. 6. Plot of temperature dependence of $\chi_m T$ and χ_m^{-1} for compound 5.

In order to estimate the strength of the antiferromagnetic exchange interactions, a phenomenological approach is used and the phenomenological equation is [49–51]:

$$\chi T = A \exp(-E_1/kT) + B \exp(-E_2/kT)$$

Herein, $A+B$ equals the Curie constant, and E_1 , E_2 represent the “activation energies” corresponding to the spin-orbit coupling and the antiferromagnetic exchange interaction. The obtained values $A+B=3.26$ cm³ mol⁻¹ K and $E_1/k=59.38$ K are consistent with those given in the literature for the Curie constant ($C=2.8$ – 3.4 cm³ mol⁻¹ K) and for the effect of spin-orbit coupling and site distortion (E_1/k of the order of 100 K). As for the value found for the antiferromagnetic exchange interaction, it is weak and the $-E_2/k=-3.51$ K.

The field dependence of the magnetization (0–8 T) measured at 2 K shows a rapid increase from zero field to 4 T (Fig. S9), and then gradually increase to $2.3 N\beta$ at 8 T, smaller than the saturation value $3.0 N\beta$ for one octahedral Co(II) ions with $S=3/2$ and $g=2.0$ [52], consistent with the observed antiferromagnetic behavior. The weak antiferromagnetic behavior may go through the carboxylate *syn-anti* bridges along the $(-\text{OCO}-\text{Co}-)_n$ chains [53,54], as well may operate through the inter-layer and intra-layer hydrogen bonding interactions [55].

4. Conclusion

In summary, under different hydrothermal conditions, we have obtained five compounds, in which the V-shaped ligand H₂oba adopts diverse coordination modes and as a result, the compounds present different dimensional structures. 1 and 2 are isomorphism, featuring pillared-layer 3D motifs with oba²⁻ as pillars. The existence of hydrogen bonding interaction promotes the formation and stability of 3D networks in 3 and 5, while 4 shows 2D layers by interchain Ag–O interaction. In addition, compounds 1–5 show structure-dependent photoluminescence or magnetism.

Acknowledgments

This research is supported by the National Natural Science Foundation of China (21271025), the Natural Science Foundation of the Education Department of Henan Province (2011A150004, 12B150004), the Department of Science and Technology of Henan Province (122102210174), the State Key Laboratory of Structural Chemistry (20110008).

Appendix A. Supporting information

Supplementary data associated with this article can be found in the online version at <http://dx.doi.org/10.1016/j.jssc.2014.04.016>.

References

- [1] J.Y. Lee, O.K. Farha, J. Roberts, K.A. Scheidt, S.T. Nguyen, J.T. Hupp, *Chem. Soc. Rev.* 38 (2009) 1450–1459.
- [2] S.J. Lee, A.G. Hu, W.B. Lin, *J. Am. Chem. Soc.* 124 (2002) 12948–12949.
- [3] Z.J. Zhang, S.C. Xiang, B.L. Chen, *CrystEngComm* 13 (2011) 5983–5992.
- [4] Z. Chang, D.S. Zhang, Q. Chen, X.H. Bu, *Phys. Chem. Chem. Phys.* 15 (2013) 5430–5442.
- [5] Y.J. Cui, Y.F. Yue, G.D. Qian, B.L. Chen, *Chem. Rev.* 112 (2012) 1126–1162.
- [6] E. Colacio, M. Ghazi, R. Kivekäs, J.M. Moreno, *Inorg. Chem.* 39 (2000) 2882–2890.
- [7] M. Kurmoo, *Chem. Soc. Rev.* 38 (2009) 1353–1379.
- [8] D. Sun, Y.H. Li, H.J. Hao, F.J. Liu, Y. Zhao, R.B. Huang, L.S. Zheng, *CrystEngComm* 13 (2011) 6431–6441.
- [9] Z.R. Pan, J. Xu, X.Q. Yao, Y.Z. Li, Z.J. Guo, H.G. Zheng, *CrystEngComm* 13 (2011) 1617–1624.
- [10] C.Y. Sun, S. Gao, L.P. Jin, *Eur. J. Inorg. Chem.* 2006 (2006) 2411–2421.
- [11] P. Mahata, M. Prabu, S. Natarajan, *Inorg. Chem.* 47 (2008) 8451–8463.
- [12] X.L. Wang, C. Qin, E.B. Wang, Y.G. Li, Z.M. Su, L. Xu, L. Carlucci, *Angew. Chem. Int. Ed.* 44 (2005) 5824–5827.
- [13] X.F. Wang, Y.B. Zhang, H. Huang, J.P. Zhang, X.M. Chen, *Cryst. Growth Des.* 8 (2008) 4559–4563.
- [14] Y.Z. Zheng, G.F. Liu, B.H. Ye, X.M. Chen, *Z. Anorg. Allg. Chem.* 630 (2004) 296–300.
- [15] Y. Ma, Z.B. Han, Y.K. He, L.G. Yang, *Chem. Commun.* (2007) 4107–4109.
- [16] Z. Jin, H.Y. Zhao, X.J. Zhao, Q.R. Fang, J.R. Long, G.S. Zhu, *Chem. Commun.* 46 (2010) 8612–8614.
- [17] H.L. Wang, K. Wang, D.F. Sun, Z.H. Ni, J.Z. Jiang, *CrystEngComm* 13 (2011) 279–286.
- [18] G.M. Sheldrick, *SHELXS-97*, Program for X-ray Crystal Structure Solution, University of Göttingen, Göttingen, Germany, 1997.
- [19] G.M. Sheldrick, *SHELXL-97*, Program for X-ray Crystal Structure Refinement, University of Göttingen, Göttingen, Germany, 1997.
- [20] Y.M. Li, C.Y. Xiao, X.D. Zhang, Y.H. Xu, J.R. Li, H.J. Lun, Q. Chen, *J. Solid State Chem.* 204 (2013) 190–196.
- [21] Y.M. Li, C.Y. Xiao, X.D. Zhang, Y.Q. Xu, H.J. Lun, J.Y. Niu, *CrystEngComm* 15 (2013) 7756–7762.
- [22] B. DasGupta, R. Haidar, W.Y. Hsieh, L.J. Zompa, *Inorg. Chim. Acta.* 306 (2000) 78–86.
- [23] M.H. Zeng, Y.L. Zhou, M.C. Wu, H.L. Sun, M. Du, *Inorg. Chem.* 49 (2010) 6436–6442.
- [24] M.H. Zeng, Q.X. Wang, Y.X. Tan, S. Hu, H.X. Zhao, L.S. Long, M. Kurmoo, *J. Am. Chem. Soc.* 132 (2010) 2561–2563.
- [25] Z. Yin, Q.X. Wang, M.H. Zeng, *J. Am. Chem. Soc.* 34 (2012) 4857–4863.
- [26] M.L. Tong, S. Hu, J. Wang, S. Kitagawa, S.W. Ng, *Cryst. Growth Des.* 5 (2005) 837–839.
- [27] P. Mahata, A. Sundaresan, S. Natarajan, *Chem. Commun.* (2007) 4471–4473.
- [28] Q.R. Fang, G.S. Zhu, M. Xue, J.Y. Sun, F.X. Sun, S.L. Qiu, *Inorg. Chem.* 45 (2006) 3582–3587.
- [29] K. Nomiyama, H. Yokoyama, *Dalton Trans.* (2002) 2483–2490.
- [30] M. Kondo, Y. Irie, Y. Shimizu, M. Miyazawa, H. Kawaguchi, A. Nakamura, T. Naito, K. Maeda, F. Uchida, *Inorg. Chem.* 43 (2004) 6139–6141.
- [31] Y.M. Li, C.Y. Xiao, S. Li, Q. Chen, B.B. Li, Q. Liao, J.Y. Niu, *J. Solid State Chem.* 200 (2013) 251–257.
- [32] H.J. Hao, D. Sun, Y.H. Li, F.J. Liu, R.B. Huang, L.S. Zheng, *Cryst. Growth Des.* 11 (2011) 3564–3578.
- [33] P. Nockemann, B. Thijs, K.V. Hecke, L.V. Meervelt, K. Binnemans, *Cryst. Growth Des.* 8 (2008) 1353–1363.
- [34] B. Ding, L. Yi, Y. Liu, P. Cheng, Y.B. Dong, J.P. Ma, *Inorg. Chem. Commun.* 8 (2005) 38–40.
- [35] D.A. Dickie, G. Schatte, M.C. Jennings, H.A. Jenkins, S.Y.L. Khoo, J.A.C. Clyburne, *Inorg. Chem.* 45 (2006) 1646–1655.
- [36] Y. Xu, F. Luo, Y.X. Che, J.M. Zheng, *Inorg. Chem. Commun.* 12 (2009) 639–641.
- [37] D.Y. Wang, H.H. Zou, F.L. Hu, Y.J. Li, *Inorg. Chem. Commun.* 26 (2012) 1–6.
- [38] J.M. Zhang, A.V. Biradar, S. Pramanik, T.J. Emge, T. Asefa, J. Li, *Chem. Commun.* 48 (2012) 6541–6543.
- [39] Q.G. Zhai, X.Y. Wu, S.M. Chen, C.Z. Lu, W.B. Yang, *Cryst. Growth Des.* 6 (2006) 2126–2135.
- [40] G. Yuan, K.Z. Shao, D.Y. Du, X.L. Wang, Z.M. Su, J.F. Ma, *CrystEngComm* 14 (2012) 1865–1873.
- [41] J. Yang, J.F. Ma, Y.Y. Liu, S.R. Batten, *CrystEngComm* 11 (2009) 151–159.
- [42] J.D. Lin, X.F. Long, P. Lin, S.W. Du, *Cryst. Growth Des.* 10 (2010) 146–157.
- [43] W. Wang, W.Q. Kan, J. Yang, J.F. Ma, *CrystEngComm* 15 (2013) 3824–3834.
- [44] L.Y. Zhang, G.F. Liu, S.L. Zheng, B.H. Ye, X.M. Zhang, X.M. Chen, *Eur. J. Inorg. Chem.* (2003) 2965–2971.
- [45] G.H. Wei, J. Yang, J.F. Ma, Y.Y. Liu, S.L. Li, L.P. Zhang, *Dalton Trans.* (2008) 3080–3092.
- [46] B. Li, S.Q. Zang, C. Ji, C.X. Du, H.W. Hou, T.C.W. Mak, *Dalton Trans.* 40 (2011) 788–792.
- [47] J. Lu, J.H. Yu, X.Y. Chen, P. Cheng, X. Zhang, J.Q. Xu, *Inorg. Chem.* 44 (2005) 5978–5980.
- [48] J.M. Rueff, N. Masciocchi, P. Rabu, A. Sironi, A. Skoulios, *Eur. J. Inorg. Chem.* (2001) 2843–2848.
- [49] J.M. Rueff, N. Masciocchi, P. Rabu, A. Sironi, A. Skoulios, *Chem. Eur. J.* 8 (2002) 1813–1820.
- [50] S.C. Manna, S. Konar, E. Zangrando, K. Okamoto, J. Ribas, N.R. Chaudhuri, *Eur. J. Inorg. Chem.* (2005) 4646–4654.
- [51] Y.L. Zhou, M.C. Wu, M.H. Zeng, H. Liang, *Inorg. Chem.* 48 (2009) 10146–10150.
- [52] O. Kahn, *Molecular Magnetism*, VCH Publishers, New York, 1993.
- [53] R.L. Carlin, K. Kopinga, O. Kahn, M. Verdager, *Inorg. Chem.* 25 (1986) 1786–1789.
- [54] H.L. Wang, D.P. Zhang, D.F. Sun, Y.T. Chen, L.F. Zhang, L.J. Tian, J.Z. Jiang, Z.H. Ni, *Cryst. Growth Des.* 9 (2009) 5273–5282.
- [55] M.H. Zeng, W.X. Zhang, X.Z. Sun, X.M. Chen, *Angew. Chem. Int. Ed.* 44 (2005) 3079–3082.